

# AGS PROPOSAL

## Search for Double- $\Lambda$ Hypernuclei by Sequential Pionic Decays

### Spokespersons

**Tomokazu Fukuda**

Laboratory of Physics,  
Osaka Electro-Communication University,  
Neyagawa, Osaka 572-8530, Japan

**Adam Rusek**

Brookhaven National Laboratory, Upton NY 11973

**R. E. Chrien**

Brookhaven National Laboratory, Upton NY 11973

Revised, Sept. 27, 2001

Beam: 1.8 GeV/c  $K^-$ ;  $3 \times 10^6$   $K^-$ /spill

Beam Line: D6 and associated spectrometer

Detector: Cylindrical Detector System

Time Requested: 1000 hours production; 200 hours setup

We ask for beam time to confirm the production of doubly-strange hypernuclei reported from BNL-AGS E906 with more than 10 times higher statistics and about twice better momentum resolution than previously obtained. The goals are three in number:

- 1) to confirm the existence of  ${}_{\Lambda\Lambda}^4\text{H}$  by looking for its 2-body decay mode to the ground state of  ${}_{\Lambda}^4\text{He}$ ;
- 2) to search for other hypernuclei such as  ${}_{\Lambda\Lambda}^5\text{H}$  and other heavier A species;
- 3) to obtain a determination of the pairing energy of  $\Lambda\Lambda$ 's to an accuracy of 0.5 MeV.

# 1 Introduction

The study of  $S = -2$  ( $\Lambda\Lambda$ ) hypernuclei provides hitherto unavailable information concerning the  $\Lambda$ - $\Lambda$  force, which is important in order to understand the baryon-baryon interaction in a unified way. In particular, it is vital for its application to multi-strange systems, such as may exist in strangelets or in neutron stars.

In the core of a neutron star, where the baryon density and thus the chemical potential is high, it becomes favorable to replace neutrons by hyperons (Y). This will cause a substantial change in the equation of state as well as in the cooling mechanisms of the neutron star [1]. However this aspect of the hyperon mixing is very uncertain at present due to the lack of the knowledge of YN and, in particular, YY interactions.

The H particle[2] has been proposed as the lightest strangelet. If the H particle is deeply bound, two lambda particles in a hypernucleus will fuse to form it. Thus the existence of weakly decaying double- $\Lambda$  hypernuclei, especially the lightest species, sets the strongest constraints on the mass of the H particle. Even if the H is not bound, an H-like component may exist in double- $\Lambda$  hypernuclei, which will bring out interesting aspects of  $\Lambda$ - $\Lambda$ ,  $\Lambda$ - $\Sigma$  and  $\Xi$ -N mixing in  $S = -2$  nuclear system.

Experimental studies on double- $\Lambda$  hypernuclei are limited. In the 1960s two double- $\Lambda$  hypernuclei were reported, showing sequential decay topologies in nuclear emulsion ( $^{10}_{\Lambda\Lambda}\text{Be}$  [3] and  $^6_{\Lambda\Lambda}\text{He}$  [4]). However the event in Ref. [4] is not convincing [5]. Recently new observations were made by the KEK-E176 and KEK-E373 experiments using the emulsion-counter hybrid detector system [6, 7], where  $\Xi^-$ -particles were captured in emulsion with higher statistics than previously. The interpretation of the E176 event is not unique, however; either  $^{10}_{\Lambda\Lambda}\text{Be}$  or  $^{13}_{\Lambda\Lambda}\text{B}$ , and accordingly the extracted  $\Lambda$ - $\Lambda$  interaction energy is either  $-4.9 \pm 0.7$  MeV (repulsive  $\Lambda$ - $\Lambda$  interaction) or  $+4.9 \pm 0.7$  MeV (attractive  $\Lambda$ - $\Lambda$  interaction). Very recently it is claimed [8] that E373 found a uniquely identified double- $\Lambda$  hypernucleus,  $^6_{\Lambda\Lambda}\text{He}$ , and determined the  $\Lambda$ - $\Lambda$  interaction to be  $1.01 \pm 0.20^{+0.18}_{-0.11}$  MeV, which is rather small compared to that claimed in past experiments.

We proposed a new method to produce and study double- $\Lambda$  hypernuclei with greater abundance by using the Cylindrical Detector System (CDS) [9], constructed to detect the pions emitted in the successive weak decays of the doubly strange system. This proposal was accepted at BNL-AGS as E906

[10], and its production run took place from September to November of 1998 in the D6 beam line of the AGS. We obtained about  $0.9 \times 10^{12}$   $K^-$  on target, only about 45 % of the total requested irradiation of the E906 proposal. Nevertheless, that experiment demonstrated the usefulness of the technique and evidence of the production of  ${}_{\Lambda\Lambda}^4\text{H}$  has been obtained.

This lightest double- $\Lambda$  hypernuclear candidate is very important in view of mass limits on the H particle, and also because it serves as a testing ground for the study of the  $\Lambda\Lambda$  interaction. An exact calculation for the four-body system is now available [11]. This situation is quite analogous to the case of the deuteron and hypertriton ( ${}_{\Lambda}^3\text{H}$ ), where exact calculations have given decisive information on nucleon-nucleon and hyperon-nucleon interactions. In the present analysis of E906, however, it is difficult to get an accurate value of the mass of  ${}_{\Lambda\Lambda}^4\text{H}$  due to inadequate statistics as well as the limited momentum resolution of CDS.

We now ask for the beam time to continue this research with significant upgrades of the CDS. In the following, we describe the experimental method and the present status of the E906 analysis, outline the objectives of the research, and show how we may attain a precise value of the  $\Lambda\Lambda$  pairing energy in the mass 4 system.

## 2 E906 experiment

As the proposed experiment is basically the same as E906 with some upgrades, we summarize here the E906 experimental procedure and instrumentation. The double- $\Lambda$  hypernuclei will be produced in the  $(K^-, K^+)$  reaction, in which a  $\Xi^-$  hyperon is first formed from a proton in the target nucleus. The  $\Xi^-$  in turn may convert into a pair of  $\Lambda$ 's by interaction with a proton, either in the nucleus in which it was produced or by subsequent interaction with a neighboring nucleus. The two  $\Lambda$ 's will be trapped in a nucleus with some probability, resulting in a formation of double- $\Lambda$  hypernuclei. The observational procedure used was the detection of pairs of decay pions, each one indicating one unit of strangeness change in sequential mesonic weak decay of a  $\Lambda\Lambda$  system. The pions are tracked in the Cylindrical Detector System (CDS), comprised of cylindrical drift chambers in a solenoidal magnetic field surrounding a beryllium target.

E906 was carried out at the AGS D6 line [12], using the beamline and its

associated spectrometer to momentum-analyze the incoming  $K^-$  and outgoing  $K^+$ , respectively. The setup, with the exception of the target region, is identical to that previously employed in several double strangeness experiments, and has been extensively described in the literature [13]. The CDS is a cylindrical detector system consisting of a solenoidal magnet (0.5 T), the volume of which is filled with a system of drift chambers surrounded by an azimuthally segmented hodoscope [9]. A schematic drawing of the CDS is shown in Fig.1. The chamber materials were chosen to minimize multiple scattering along the path from the beryllium target (1.27 cm high, 5.08 cm wide and 15.24 cm thick) at the center of the CDS to the hodoscope at its outer radius (30 cm). The chamber volume is subdivided into 12 layers of two different types – axial layers, whose sense wires are parallel to the beam axis, and stereo layers, with sense wires inclined at angles ranging from 3.4 to 5.8 degrees.

The magnetic field is uniform to 0.5 % throughout the enclosed volume (30 cm radius, 100 cm length) and is anti-parallel to the beam direction. Most of the chamber volume is devoted to tracking the out-of-beam particles. The component of the momentum in the x-y plane (transverse momentum,  $P_t$ ) was deduced from the curvature of the track in that plane. The projection of the track on the z-axis was obtained from stereo-wire-layer information in the drift-chamber volume. Combining these measurements we obtained the total momentum vector. The hodoscope(CDH) was used for both triggering and time-of-flight measurement within the CDS, so that complete particle identification by charge and mass was achieved.

Data were also recorded with a series of spatially separated polyethylene slabs to study vertex reconstruction and resolution using  $(\pi^-, p)$  elastic scattering at 450 MeV/c. The targets were used for momentum calibration, using  $\Sigma^+$  decay from the  $p(K^-, \pi^-)\Sigma^+$  reaction. The momentum so measured, at 185 MeV/c, confirmed the design value to an accuracy of 1 MeV/c. The momentum resolution of CDS was also calculated over the range 20 to 300 MeV/c by simulations which included tracking chamber resolution (250  $\mu$ m rms), multiple scattering, and target thickness correction uncertainties due to tracking errors. The overall 3-dimensional positional accuracy for vertex determination was estimated as 3 mm. From all these contributions to the resolution, a rms uncertainty of 4 MeV/c, at 100 MeV/c, was predicted. This result was confirmed by fitting the  $\Sigma^+$  decay mentioned above, as well as by fitting decays of the twin  $\Lambda$  hypernuclei  ${}^3_\Lambda\text{H}$  and  ${}^4_\Lambda\text{H}$  at 114 and 133 MeV/c,

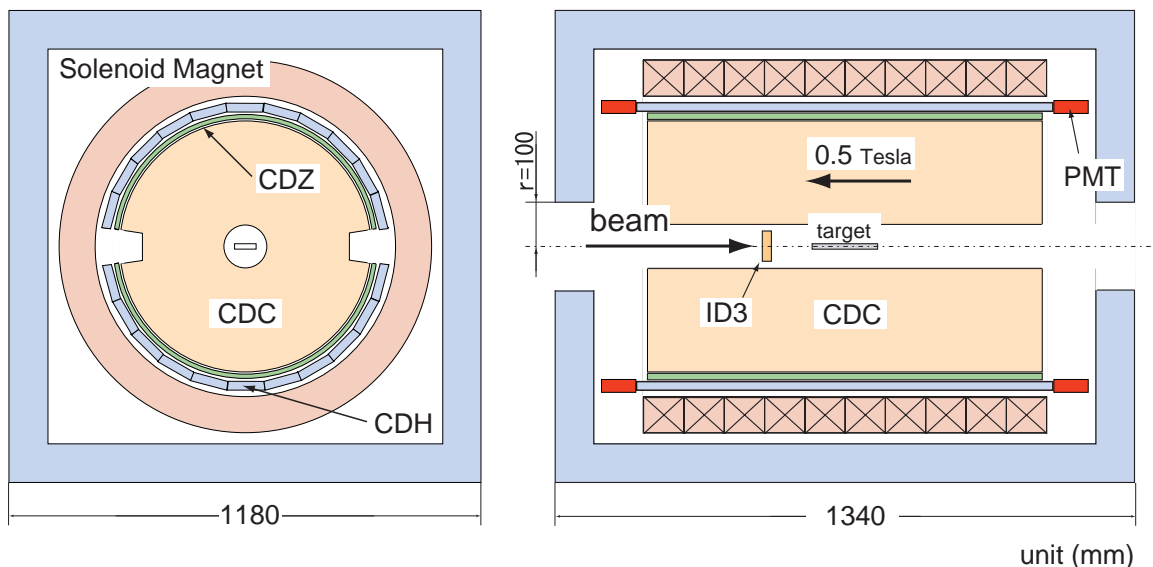


Figure 1: Schematic front and side views of the CDS; ID3, CDC, and CDZ refer to chambers, PMT to photomultipliers, and CDH to a scintillation hodoscope.

respectively, in the Be target. The reconstruction efficiency of the CDS was typically in the range of 65 %.

The physics data was taken in two trigger modes; one was an unbiased ( $K^-$ ,  $K^+$ ) trigger with a prescale value of 20 and the other was CDH-related ( $K^-$ ,  $K^+$ ) trigger, where at least one hit on CDH was required. During the production run in 1998 the typical  $K^-$  flux at 1.8 GeV/c was  $2.0 \times 10^6$  per spill, with a  $K^-/\pi$  ratio of 0.5. An integrated flux of  $0.9 \times 10^{12}$  kaons on the beryllium target was accumulated, leading to  $1.1 \times 10^5$  triggers.

### 3 E906 Results

The data set on which the analysis is based consists of those events in which  $\Xi^-$  production from a beryllium target took place in coincidence with the detection of two negatively-charged tracks in the CDS. A loose chi-square-per-degree-of-freedom cut of  $<4$  was imposed on the tracking. This set was

further subjected to the requirement that the distance of closest approach (DCA) between the two tracks be less than 2.0 cm, and that the associated vertex be within the target.

The pion pairs were ordered with respect to their measured momenta; the pion with the higher momentum is labeled “ $\pi_H$ ” while the one with the lower is labeled “ $\pi_L$ ”. Since  $\pi^-$ ’s emitted into small polar angles are almost entirely of fast  $\Xi^-$ -decay origin, event pairs with  $\pi_H$  polar angles less than  $60^\circ$  were rejected. A further restriction which is important in background reduction is the rejection of all events whose  $\Xi$  “missing mass” exceeds  $1343 \text{ MeV}/c^2$ . This cut removed about half of the remaining events – those corresponding to high excitations in the quasi-free  $\Xi$  spectrum.

Figure 2 contains a two-dimensional scatter plot of the pion pair events, obtained as described above, binned in  $3 \text{ MeV}/c$  cells. The box size shown is proportional to the cell population.

The main source of background for the two  $\pi^-$  data is expected to come from  $\Xi^-$  decay, which results in  $p + \pi^- + \pi^-$  about 64% of the time (the rest of the time the final state includes neutral particles). An extensive simulation of quasifree  $\Xi^-$  production in the CDS was carried out. The quasifree  $\Xi^-$  events appear in our experiment as two negative tracks in the CDS when the proton is not detected, either because it is outside the geometric acceptance or, for low momentum  $\Xi^-$ ’s, because it never leaves the target. The events in which all three tracks were detected were limited to about 800 in number, about 5 % of the two  $\pi^-$  set (before applying cuts as described above). They were analyzed to compare to our simulation which includes the geometry and response of the CDS. The shape comparison was satisfactory, and the simulated spectrum magnitude was fixed by the three-track data. The simulation then provided a reliable measure of the  $\Xi^-$  background magnitude and shape in the two-track data.

The pion spectrum will exhibit a sharp peak in a two-body decay from a system at rest, or nearly at rest, such as a double or single- $\Lambda$  hypernucleus. A correlated signal, which appears as such a peak in both pion spectra, is interpreted as a pair of single- $\Lambda$  hypernuclei if the momenta match known decays of single- $\Lambda$  systems. It is regarded as a candidate for a double- $\Lambda$  hypernucleus when only one of the lines matches a known decay momentum [14, 15, 16, 17, 18]. Fig. 3, adapted from Reference [14], indicates where known single  $\Lambda$  hypernuclear lines are expected as well as where  $\Lambda\Lambda$  decay lines are anticipated as a function of the  $\Lambda\Lambda$  pairing energy,  $\Delta B_{\Lambda\Lambda}$ .

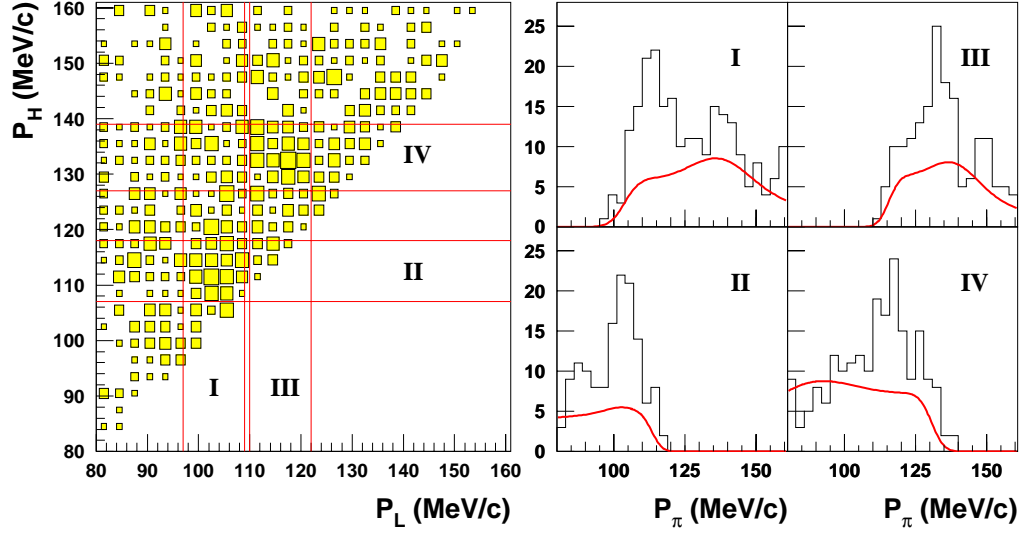


Figure 2: The momenta of  $\pi_H$  and  $\pi_L$ , in MeV/c, plotted against each other (left). The event concentration associated with the  ${}^4_{\Lambda\Lambda}\text{H}$  doubly-strange hypernucleus is located near (114,104). The plots on the right, I and II, are projections on the y and x axis, respectively, with the indicated limits. The projections shown in III and IV are attributed to  ${}^4_{\Lambda}\text{H}$  and  ${}^3_{\Lambda}\text{H}$ . The overlaid curves for I-IV are the measured quasi-free  $\Xi^-$ -decay backgrounds, normalized to the expected number of such events in the data.



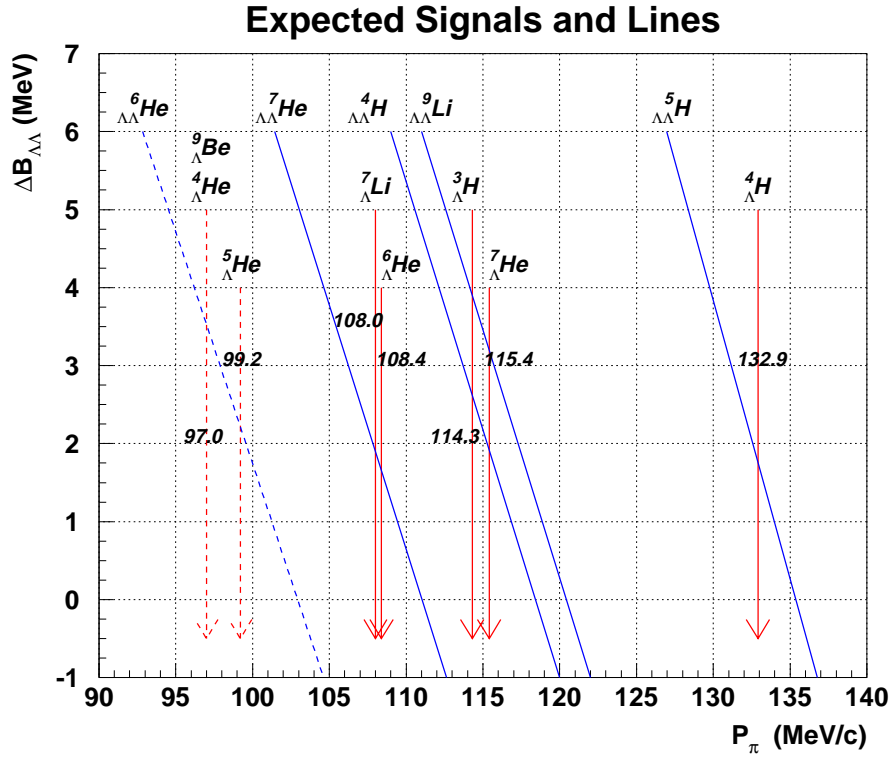


Figure 3: The decay momenta for singly and doubly strange hyperfragments for the light systems expected to be produced in this experiment. Inclined lines reflect the dependence on the assumed  $\Lambda\Lambda$  pairing energy.

Inspection of the plot indicates two regions of event concentration; one near (104,114) and one near (114,133) in the pion momentum axes. The right hand side of the figure shows projections of the data regions in the indicated bands of 12 MeV/c width (3 sigma in CDS resolution) on the  $P_H$  and  $P_L$  axes. Histogram (I) displays the higher momentum pion distribution with the lower pion momentum between 97 and 109 MeV/c, while (II) shows the lower pion momentum distribution, with the upper pion cut between 107 and 119 MeV/c. The event concentration projected in I and II we attribute to  ${}_{\Lambda\Lambda}^4\text{H}$  as explained below, while those projected in III and IV are attributed to the decays,

$${}_{\Lambda}^3\text{H} \rightarrow {}^3\text{He} + \pi_L^- \quad (114.3 \text{ MeV}/c) \quad (1)$$

$${}_{\Lambda}^4\text{H} \rightarrow {}^4\text{He} + \pi_H^- \quad (132.9 \text{ MeV}/c) \quad (2)$$

The existence of these twin hypernuclei is evidence that  $\Xi^-$ 's of appreciable kinetic energy are initiating reactions. Also indicated in the projected spectra I to IV are the appropriate backgrounds from quasi-free  $\Xi^-$  production, determined from the three particle tracks as described above. A clear excess of signal over  $\Xi^-$  background is observed in these spectra.

We direct attention to two structures in Figure 2, a relatively wide peak centered near 114 MeV/c in 2-I, and the correlated narrow low-momentum peak near 104 MeV/c in 2-II. The latter prominent peak has no clear explanation in the literature. It is the conjunction of this feature with the wide peak in 2-I that points strongly to the existence of  ${}_{\Lambda\Lambda}^4\text{H}$  in our data sample. The broadening near 114 MeV/c is attributed to the presence of more than a single contribution and the peak at 104 MeV/c to a particular decay mode of the doubly-strange hypernucleus. We develop this argument as follows.

Consider the following possible sequences, some of which are combinations of single  $\Lambda$  decays. The decay momenta, known from emulsion experiments to typically better than 1 MeV/c, are near those of the correlated peaks. These are listed below as processes (3,4) and (5,6).

$${}_{\Lambda}^3\text{H} \rightarrow {}^3\text{He} + \pi_H^- \quad (114.3 \text{ MeV}/c) \quad (3)$$

$${}_{\Lambda}^6\text{He} \rightarrow {}^6\text{Li} + \pi_L^- \quad (108.4 \text{ MeV}/c) \quad (4)$$

$${}^3_{\Lambda}\text{H} \rightarrow {}^3\text{He} + \pi_H^- \quad (114.3 \text{ MeV}/c) \quad (5)$$

$${}^4_{\Lambda}\text{H} \rightarrow {}^3\text{H} + p + \pi_L^- \quad (\sim 98 \text{ MeV}/c) \quad (6)$$

In (4) is listed a possible two-body decay of  ${}^6_{\Lambda}\text{He}$  which might populate low-lying excited states of  ${}^6\text{Li}$  as well as the ground state. However this two-body decay has not been reported in the standard compilations because of inherent difficulties in handling two-prong events [16]. Most of the strength in (4) is expected to go to highly excited states of  ${}^6\text{Li}$  resulting in three-body decays with  $\pi^-$  momenta below 100 MeV/c [20]. Thus this decay cannot explain the sharp feature near 104 MeV/c in Figure 2-II. Similarly, the three-body decay of (6) is well-below the sharp structure of Figure 2-II, although it might account for some background below that peak.

The only other possibilities are sequential decays of  ${}^4_{\Lambda\Lambda}\text{H}$ ,

$${}^4_{\Lambda\Lambda}\text{H} \rightarrow {}^4_{\Lambda}\text{He} + \pi_H^- \quad (\sim 114 \text{ MeV}/c) \quad (7)$$

$${}^4_{\Lambda}\text{He} \rightarrow {}^3\text{He} + p + \pi_L^- \quad (97 \text{ MeV}/c) \quad (8)$$

and in particular, a decay into a possible excited state of  ${}^4_{\Lambda}\text{He}$ ,

$${}^4_{\Lambda\Lambda}\text{H} \rightarrow {}^4_{\Lambda}\text{He}^* + \pi_L^- \quad (\sim 104 \text{ MeV}/c) \quad (9)$$

$${}^4_{\Lambda}\text{He}^* \rightarrow {}^3_{\Lambda}\text{H} + p \quad (10)$$

$${}^3_{\Lambda}\text{H} \rightarrow {}^3\text{He} + \pi_H^- \quad (114.3 \text{ MeV}/c). \quad (11)$$

The resonance in (9,10) has not been observed experimentally, but its existence is indeed plausible [21]. The light hypernucleus,  ${}^4_{\Lambda}\text{He}^*$ , when in the resonant state of interest, is rather extended spatially. A narrow, P-wave, resonance can be modeled in a reasonably sized potential, whose depth is constrained by the known energies of the ground state  $(0^+, 1^+)$  pair of levels. The emission into this quasi three-body decay is [17] expected to constitute more than half the total decay of the parent  ${}^4_{\Lambda\Lambda}\text{H}$ , and the calculated widths [21] permit sufficient competition with  $\Lambda$  escape from  ${}^4_{\Lambda}\text{He}^*$ . The determination of a separable peak momentum for the first of these decay chains would constitute a measurement of  $\Delta B_{\Lambda\Lambda}$  in  ${}^4_{\Lambda\Lambda}\text{H}$ .

The signals from systems (3,4) and (5,6) are thus small or virtually nonexistent, and the limited statistics of the present data set preclude discussion

of possible small signals. The absence of a strong signal from  ${}_{\Lambda\Lambda}^5\text{H}$ , which we originally expected to dominate the spectrum near 135 MeV/c[14], compels us to reexamine the possible mechanisms driving these systems, from production to fragmentation.

A simple model which views the  ${}^9\text{Be}$  nucleus as consisting of a pair of  $\alpha$  particles ( i. e. a  ${}^8\text{Be}$  nucleus) held together by a weakly bound neutron is suggested. A  $\Xi^-$  can be considered incident on one of the  $\alpha$ 's, the other  $\alpha$  and the neutron acting essentially as spectators. The final state reached will depend on the kinetic energy of the incident  $\Xi^-$ ; most collisions with appreciable energy will result in the ejection from the struck  ${}^4\text{He}$  of a neutron, as well as the conversion of one of the protons, with the  $\Xi^-$ , into two  $\Lambda$ 's. The end product, if an  $S = -2$  nucleus at all, is then more likely to be  ${}_{\Lambda\Lambda}^4\text{H}$  than  ${}_{\Lambda\Lambda}^5\text{H}$ . Even if the initiating  $\Xi^-$  is at rest, the Q value is probably too large to permit the copious formation of  ${}_{\Lambda\Lambda}^5\text{H}$ . Of course, more massive compound nuclei and hence more massive hypernuclei can result from nuclear interactions of  $\Xi^-$ 's, but not at rates discernible in the present data set.

The production rate of  $\Lambda\Lambda$  hypernuclei may be estimated from inspection of Fig.2-II. The peak in that figure contains about 34 events above a background, one-half of which is attributable to quasifree cascade decays. After suitable corrections for tracking and cut efficiencies, and CDS solid angle acceptance, we estimate a production of about 400  ${}_{\Lambda\Lambda}^4\text{H}$  events, or about .0048 per quasi-free cascade produced in our experiment. Since the estimate relies on assumptions about the unknown neutral mode decay fractions of the members of the production chain, it should be considered as only an order-of-magnitude estimate.

The observation of numerous  $\Lambda\Lambda$  hypernuclei in this experiment argues against the existence of an  $S=-2$  dibaryon with a mass less than a few MeV below that of a  $\Lambda\Lambda$  system. We observe the weak decay of such a system which presumably could not compete against the strong  $\Lambda\Lambda \rightarrow H$  reaction.

In order to validate the above conclusions, we have performed extensive checks on the performance of the CDS, and the capability of our analysis procedure. These were compared to the collection of 3-track events recorded in the E906 production run. Some of these checks are demonstrated here. The results are best summarized by reference to the following three figures (Fig. 4, Fig. 5, and Fig. 6) which demonstrate our ability to identify and track the  $\Xi$  and  $\Lambda$  hyperons. The first of these, Fig.4 shows the invariant mass of the  $\Lambda$  hyperon reconstructed from the  $\Xi$  decay, while the second

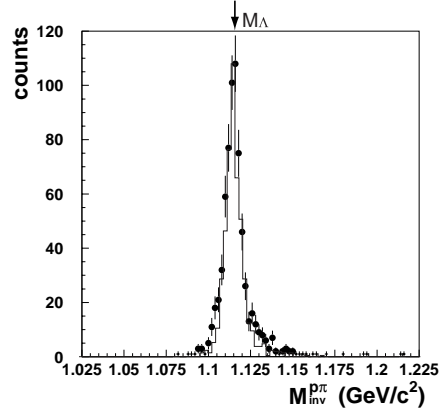


Figure 4: The invariant mass spectrum obtained in the CDS between proton and the  $\pi^-$ . The peak corresponds to the  $\Lambda$

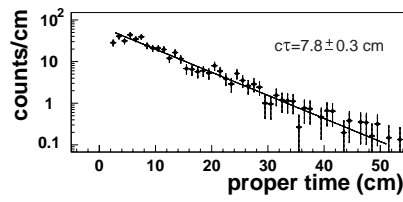


Figure 5: The proper time distribution of the reconstructed  $\Lambda$

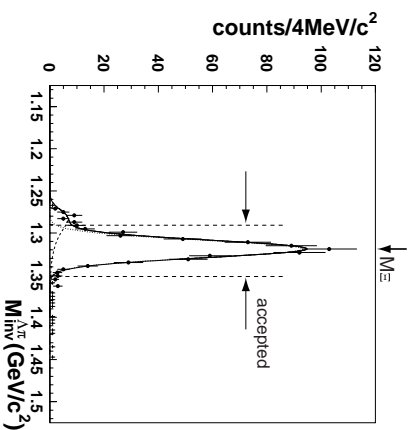


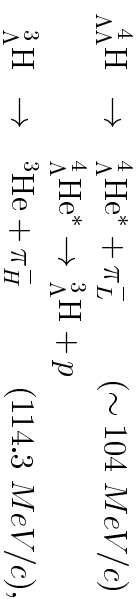
Figure 6: The invariant mass distribution between the reconstructed  $\Lambda$  and the decay  $\pi^-$ .

figure, Fig.5 shows the  $\Lambda$  lifetime derived from the reconstruction. Finally, Fig.6 demonstrates that we get the correct mass for the  $\Xi$  hyperon which initiates the sequential pionic decays.

## 4 The proposed research

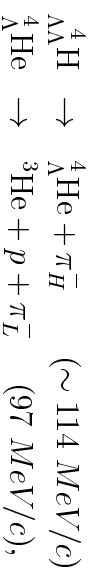
Having established the method for production and identification of  $\Lambda\Lambda$  systems in quantity, we now turn to the problem of arriving at a precise measurement of the  $\Lambda\Lambda$  pairing energy,  $\Delta_{B\Lambda\Lambda}$ . To that end, we propose:

(1) to confirm the signal around (104 MeV/c, 114 MeV/c), which is interpreted as



with better statistics, better momentum resolution of decay pions and less background.

(2) to identify the two-body decay mode,



in order to get the pairing energy of the  $\Lambda$ 's within the mass 4 double- $\Lambda$  hypernucleus, i. e. a deuteron plus two  $\Lambda$ 's.

We carried out a Monte Carlo simulation in order to evaluate the overall improvement to be expected in the CDS. A description of the simulation is given in Appendix B; the program is based on the well-studied analysis program developed and checked for E906. This simulation when applied to the conditions under which E906 was run, predicted a momentum resolution of 4.3 MeV/c (rms) at 100 MeV/c, which is consistent with the E906 results.

In the following, we describe several significant improvements to help us meet the goals of an order-of-magnitude higher statistics and an improvement of nearly a factor of two in the momentum resolution of CDS. Each improvement has been evaluated by comparison to the Monte Carlo simulation of CDS.

To improve the statistics, we will increase the acceptance of the forward  $K^+$  by a factor of about two by moving the beryllium target 30 cm downstream of the CDS center. The calculated increase takes account of the  $(K^-, K^+)$  reaction kinematics and the calculated angular distribution for double strangeness production[19]. In doing so, the efficiency for two decay pion detection will be slightly decreased (by 7 %) in this target geometry. By placing the  $^9\text{Be}$  target downstream, the background pions from  $\Xi^-$  decays in flight will be also be reduced, however, because those pions are preferably emitted to the forward direction.

The second crucial point is an improved momentum resolution of CDS; this may enable us to distinguish the two-body decay mode of  $^4_{\Lambda\Lambda}\text{H}$  from the neighboring  $^3_{\Lambda}\text{H}$  decay. We will install a vertex detector, internal to the CDS and near the target, to provide a much better vertex determination in the target region. This will improve the effective momentum resolution by reducing the ambiguity in the projection of the track on the z-axis as well as in the energy-loss correction in the target due to the error of the target path-length estimate. The vertex chamber will also reduce the background from cascade decay. The imposition of a more accurate distance of closest approach (DCA) between the two coincident tracks will reduce the background from unrelated pionic cascade decays, without affecting the true double- $\Lambda$  signal.

An internal vertex tracker has been designed. The structure consists of one layer of a cylindrical MWPC with a cathode readout (see Appendix C). Fig. 7 shows distance-of-closest-approach (DCA) distributions. This figure shows a comparison of the effectiveness of the cut that can be applied to the

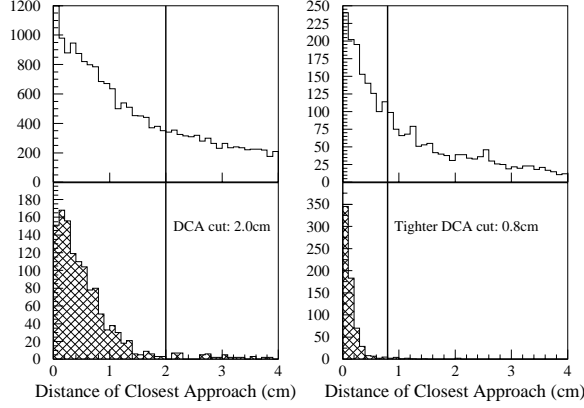


Figure 7: A comparison of the DCA spectrum obtained before (top) and after (bottom) the addition of the vertex chamber described in appendix B

new data. On the basis of the figure, we will use a DCA cut of 0.8 cm, to be compared to the previously used 2.0 cm. A study the mometum resolution as a function of the vertex chamber spatial resolution indicates that a modest spatial resolution of  $300 \mu\text{m}$  is adequate, since at this level the momentum resolution is limited by multiple scattering in the Be target.

A straightforward way to improve the momentum resolution is to increase the current of the solenoidal magnet of CDS by 30 % ( field strength of 6.5 kG instead of the present 5 kG) so as to increase the bending power. The use of a thinner  $^9\text{Be}$  target (0.8 cm high) and a higher fraction of He gas for CDC chamber (He : Ethane = 80 : 20 instead of 50 : 50 for E906) will further reduce the energy-loss and multiple scattering in CDC.

The effect of a stronger field in the CDS was studied using TOSCA, a universally-used 3-dimensional code. The program simulated the effect of increasing the magnet current on the uniformity of the magnetic field as well as for the gain of the photomultipliers of CDH. It was found that an increase of 30 % will not cause a significant deterioration of field quality within the effective volume of the tracking chambers. The loss of PMT output is not important since E906 had more than an adequate signal for pion detection.

The simulation incorporating the above modifications has been performed, and it shows that the resolution (at 100 MeV/c) will be improved to from the present 4.0 MeV/c (rms) to 3.0 MeV/c (rms) when only the vertex chamber is incorporated and to 2.5 MeV/c (rms) when, in addition, the magnetic field is raised to 6.5 kG.



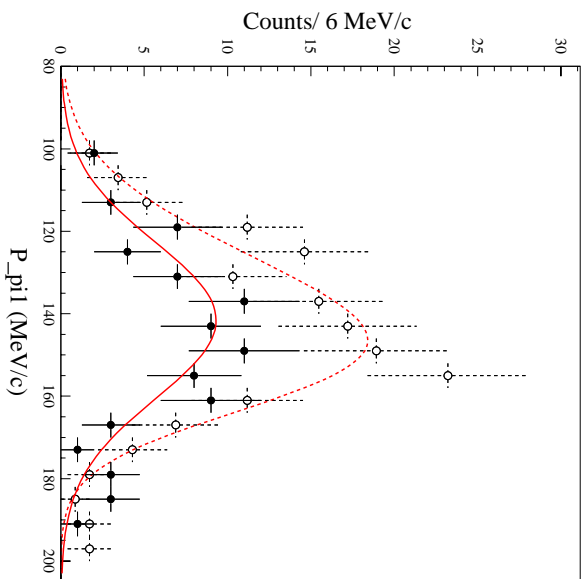


Figure 8: The simulation result for the 2-pion background spectrum resulting from cascade decay. The improvement shown by the dark circles as compared to the open circles results from a DCA cut change from 2.0 to 0.8 cm, taking advantage of the improved tracking afforded by the vertex chamber.

With all the improvements discussed included, the Monte Carlo simulation was applied to the expected signal for the 2-body and 3-body decays of  ${}^4_{\Lambda\Lambda}\text{H}$ . The object was to see how accurately the pairing energy between two  $\Lambda$ 's,  $\Delta B_{\Lambda\Lambda}$ , could be determined. From E906 we know that the pion expected from the 2-body decay mode of  ${}^4_{\Lambda\Lambda}\text{H}$  is close to the one from the decay of  ${}^3_{\Lambda}\text{H}$ , arising mostly from the decay chain of (9) - (11) for the same double- $\Lambda$  hypernucleus,  ${}^4_{\Lambda\Lambda}\text{H}$ .

At first we simulated the cascade background with the improved experimental conditions. The simulation program is the same as used for E906 and it reproduced well the E906 data for the three-track events, which come entirely from the cascade decay, in magnitude and shape. We incorporated into this program peak fitting to predict how accurately the pairing energy is determined. We generated a fixed peak corresponding to the known decay of  ${}^3_{\Lambda}\text{H}$ , i.e. 114.3 MeV/c, with the rms resolution of 2.8 MeV/c, expected for 114 MeV/c. We also generated peaks of various momenta with that resolution, simulating the two-body decay mode of  ${}^4_{\Lambda\Lambda}\text{H}$ . A typical example of the simulated peaks as well as background is shown in Fig.9.

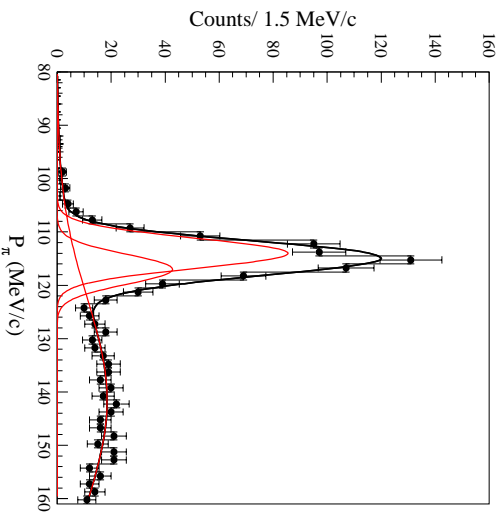


Figure 9: A simulated response to the two components situated near 114 MeV/c, showing an assumed separation of one sigma in CDS momentum resolution, i. e. 2.7 MeV/c. This figure shows the difficulty in determining the separation by least squares curve fitting.

One sees a significant improvement of the signal to background ratio as compared to E906 data (see Fig.2-1), which is due to the better target geometry as well as the tighter DCA cut. Figure 9 however, illustrates the difficulty of isolating the two components contributing to the interesting region near 114 MeV/c: the hypertriton,  ${}^3\text{H}$ , decay from the crucial  ${}_{\Lambda\Lambda}{}^4\text{H}$  decay. In the simulation we have assumed a 2:1 ratio of  $\Lambda\Lambda$  signal to the interfering hypertriton signal, and a momentum separation of 2.7 MeV/c (about 1 sigma in our resolution function). It is clear that while one might deduce the presence of the interference from a peak broadening, the extraction of an accurate  $\Lambda\Lambda$  energy will be difficult, even with this resolution improvement.

In order to achieve a pairing energy measurement, it will be necessary to turn to the lower pion momentum determination near 100 (MeV/c). In Fig. 11 are four plots displaying the results of a Monte Carlo simulation. Both the high and the low momentum pions were produced, modeling the decay chains (7),(8) and (9),(11) with the ratio of (7) to (9) being 1:2 (as in Fig. 9). On the left hand side are the spectra of the high momentum and the low momentum pions. Also overlaid are the individual contributions of decay chain (7),(8) (in red, or the *smaller* one in each case), and decay chain

(9),(11) (in blue, or the *larger* one in each case). Because (8) is a 3-body decay, the resulting momentum spectrum is low and has an extended tail down below 80 MeV/c. Thus, a cut on the lower-momentum pion at about 98 MeV/c can separate the two decay chains in the higher-momentum pion spectrum, as illustrated in the right hand side of Fig. 11. The separation of the two contributions in the high-momentum pion spectrum is unknown, and was arbitrarily picked here to be about 3 MeV/c. Even if both are at 114 MeV/c, they can be separated by the low-momentum pion cut.

Further minor improvements will be made to increase data-taking efficiency. Electronic circuits as well as the data acquisition system are being upgraded; we are preparing a new preamplifier for CDC consisting of a combined chip of a preamplifier and a discriminator in order to avoid an oscillation problem which troubled us during the 1998 run. This preamp has already been tested and is ready for production under Japanese funding. We have already installed, for E930, a high-rate capability DAQ for the FY2001 run at D6 line. It is readily adaptable for a CDS using the high-intensity  $K^-$  beam at D6 line. This system can easily accommodate 250 triggers/spill, the anticipated rate for this proposal.

In the 1998 E906 run we got  $0.9 \times 10^{12}$  kaons under the condition that the average  $K^+$  beam intensity was  $1.5 \times 10^6$  per spill (2.0 sec out of a 4.3 sec period) for a proton intensity of 7 Tp per spill on the D6 production target for 450 hours. We wish to take advantage of the maximum production target capability provided by the AGS, and we now request the maximum allowed irradiation rate of 15 Tp/spill and a 47% duty factor. For 1000 hours, we will obtain  $(15/7) \times (1000/450) \times (2.4) \times (1/1.07) = 10.7$  times more pion coincident events than obtained in E906. This request asks for an additional 200 hours in setup and calibration time, for a total request of 1200 hours.

## 5 Summary

The study of double- $\Lambda$  hypernuclei ( $S = -2$ ) provides hitherto unavailable information concerning the  $\Lambda$ - $\Lambda$  force, which is important in order to understand the baryon-baryon interaction in a unified way, and in particular for its application to multi-strange systems, such as hyperon-mixed neutron star and strangelet. However the experimental studies have been limited.

We proposed a new method to study double- $\Lambda$  hypernuclei (E906) by

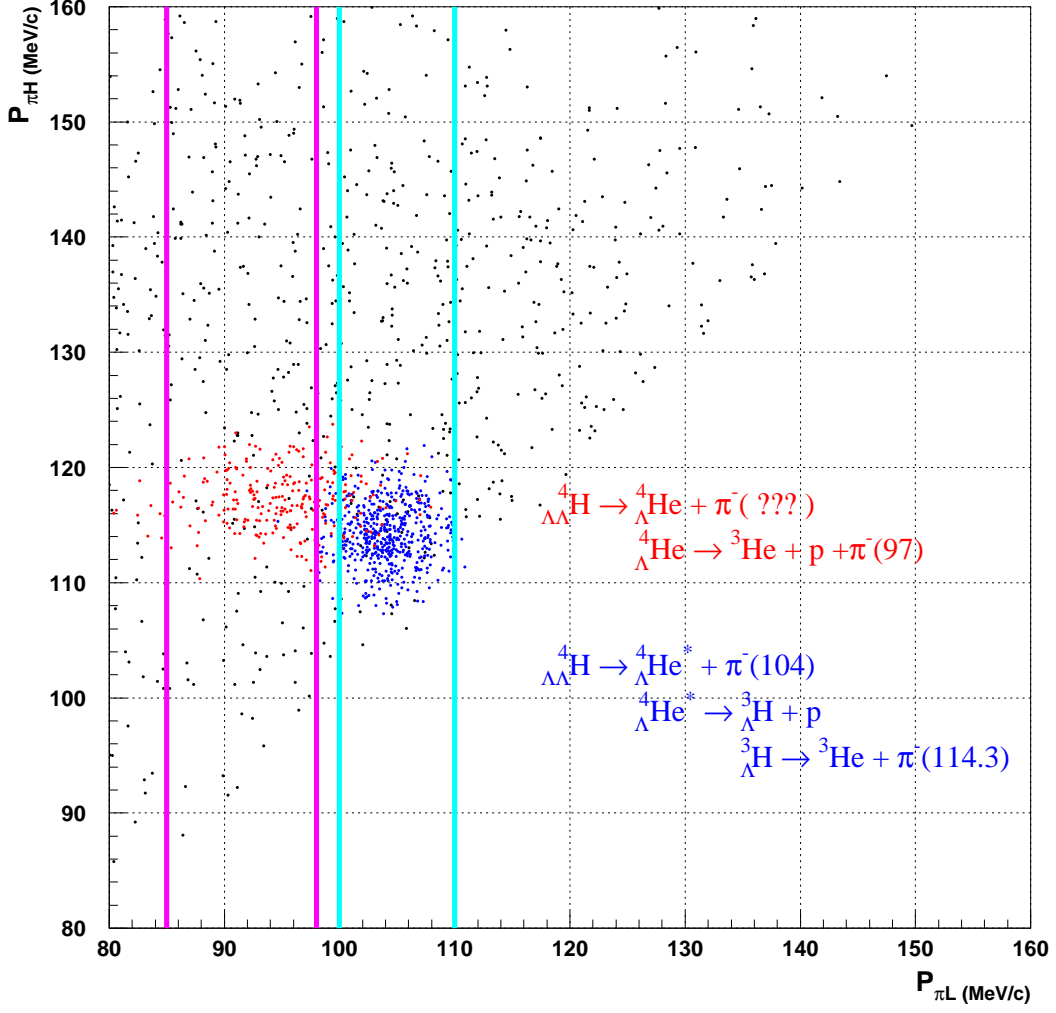


Figure 10: A 2-d plot of the high momentum pion against the low momentum pion according the simulation incorporating the higher momentum resolution, vertex resolution, and increased count rate outlined in the text. The left cut corresponds to the top equation, the right to the bottom equation.

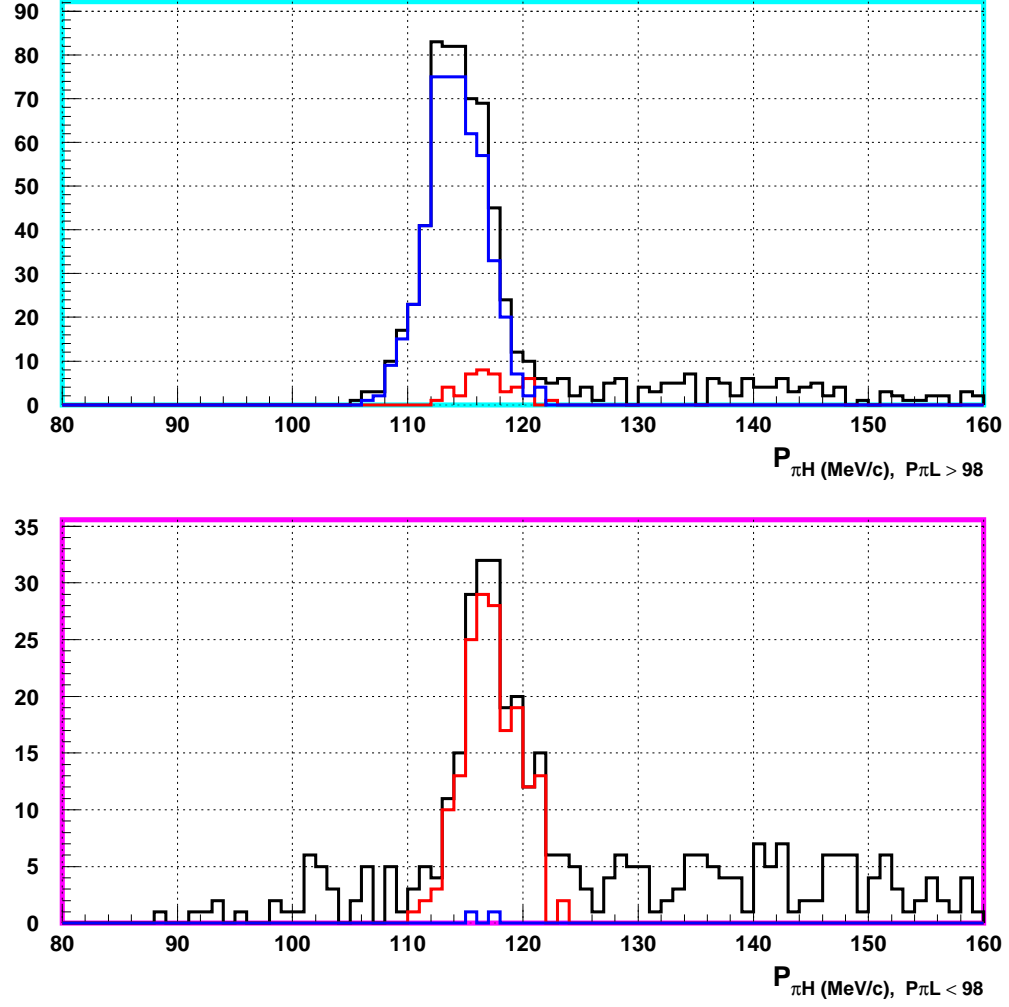


Figure 11: The spectra corresponding to the cuts of the previous figure. The intent of these cuts is to separate the two- and three-body decays of  ${}^4_{\Lambda\Lambda}\text{H}$ . Their contributions are seen to be separated by these cuts, when the upper right figure is compared to the lower.

using the Cylindrical Detector System (CDS). The initial operation of E906 was carried out in the period September to November of 1998 in the D6 beam line of the AGS. Although we got about  $0.9 \times 10^{12}$   $K^-$  on target, or only about 45 % of the total requested irradiation of the E906 proposal, that experiment has demonstrated the usefulness of this technique and an evidence of the production of  ${}_{\Lambda\Lambda}^4H$  has been obtained. In the present analysis, however, it is difficult to get an accurate value of the mass of  ${}_{\Lambda\Lambda}^4H$  due to statistics as well as a limited momentum resolution of CDS for decaying pions.

Based on that study we now ask for the beam time to reconfirm the production of  ${}_{\Lambda\Lambda}^4H$  with more than 10 times higher statistics and about twice better momentum resolution of decay pions and to get its binding energy or pairing energy of the  $\Lambda$ 's within the mass 4 double- $\Lambda$  hypernucleus, i. e. a deuteron plus two  $\Lambda$ 's with an accuracy of at least 0.5 MeV. We request 1000 hours at 15 Tp for production and 200 hours at 5 Tp for setup and calibration. The upgrade of CDS has been started by the approved budget in Japan.

## A The Collaboration

J. K. Ahn<sup>13</sup>, S. Ajimura<sup>10</sup>, H. Akikawa<sup>7</sup>, B. Bassalleck<sup>9</sup>, A. Berdoz<sup>2</sup>, D. Carman<sup>2</sup>, R. E. Chrien<sup>1</sup>, C. A. Davis<sup>8,14</sup>, P. Eugenio<sup>2</sup>, H. Fischer<sup>3</sup>, G. B. Franklin<sup>2</sup>, J. Franz<sup>3</sup>, T. Fukuda<sup>15</sup>, L. Gan<sup>4</sup>, H. Hotchi<sup>12</sup>, A. Ichikawa<sup>7</sup>, K. Imai<sup>7</sup>, S. H. Kahana<sup>1</sup>, P. Khaustov<sup>2</sup>, T. Kishimoto<sup>10</sup>, P. Koran<sup>2</sup>, H. Kohri<sup>10</sup>, A. Kourepin<sup>6</sup>, K. Kubota<sup>12</sup>, M. Landry<sup>8</sup>, M. May<sup>1</sup>, C. Meyer<sup>2</sup>, Z. Meziani<sup>11</sup>, S. Minami<sup>10</sup>, T. Miyachi<sup>12</sup>, T. Nagae<sup>5</sup>, J. Nakano<sup>12</sup>, H. Outa<sup>5</sup>, K. Paschke<sup>2</sup>, P. Pile<sup>1</sup>, M. Prokhabatilov<sup>6</sup>, B. P. Quinn<sup>2</sup>, V. Rasin<sup>6</sup>, A. Rusek<sup>1</sup>, H. Schmitt<sup>3</sup>, R. A. Schumacher<sup>2</sup>, M. Sekimoto<sup>5</sup>, K. Shileev<sup>6</sup>, Y. Shimizu<sup>10</sup>, R. Sutter<sup>1</sup>, T. Tamagawa<sup>12</sup>, L. Tang<sup>4</sup>, K. Tanida<sup>12</sup>, K. Yamamoto<sup>7</sup>, L. Yuan<sup>4</sup>

<sup>1</sup>Brookhaven National Laboratory, Upton NY 11973, USA.

<sup>2</sup>Department of Physics, Carnegie Mellon University, Pittsburgh PA 15213, USA.

<sup>3</sup>Department of Physics, University of Freiburg, D79104 Freiburg, Germany.

<sup>4</sup>Department of Physics, Hampton University, Hampton VA 23668, USA.

<sup>5</sup>High Energy Accelerator Research Organization (KEK), Tsukuba, Ibaraki 305-0801, Japan.

<sup>6</sup>Institute for Nuclear Research (INR), Moscow 117312, Russia.

<sup>7</sup>Department of Physics, Kyoto University, Sakyo-Ku, Kyoto 606-8502, Japan.

<sup>8</sup>Department of Physics and Astronomy, University of Manitoba, Winnipeg, MB, Canada R3T 2N2.

<sup>9</sup>Department of Physics and Astronomy, University of New Mexico, Albuquerque, NM 87131, USA.

<sup>10</sup>Department of Physics, Osaka University, Toyonaka, Osaka 560-0043, Japan.

<sup>11</sup>Department of Physics, Temple University, Philadelphia, PA 19122, USA.

<sup>12</sup>Department of Physics, University of Tokyo, Tokyo 113-0033, Japan.

<sup>13</sup>Department of Physics, Pusan National University, Pusan 609-735, Korea.

<sup>14</sup>TRIUMF, 4004 Wesbrook Mall, Vancouver, BC, Canada V6T 2A3

<sup>15</sup>Laboratory of Physics, Osaka Electro-Communication University, Neyagawa, Osaka 572-8530, Japan

## B CDS Simulation

A simulation of the detection of decay particles in the CDS was created with the use of the CERN program GEANT 3.2.1[22]. The calculation was divided into two parts: a) the detection simulator in which hit positions and the resulting 4-momentum vectors were generated to test the CDS acceptance and geometry, and b) the signal simulator which returns the drift length for each hit cell. These generated data were fed into the tracking routines used in the CDS to evaluate the response function and the cut efficiencies[23].

Elements of the detector systems were surveyed to an accuracy of better than 500  $\mu$ meters, and in the simulation, the effect of positional uncertainties was estimated by varying positions with a tolerance band of that amount. The solenoidal field was mapped and showed uniformity of better than 0.5%. For simulating the  $(K^-, K^+)$  reaction on beryllium, harmonic oscillator wave functions with parameters  $\alpha=1.46(2.1)$  and  $b=1.65(1.65)$  for the proton(neutron). The effect of proton binding was included by reducing the proton mass by 16 MeV in the calculation of the outgoing  $K^+$  momentum. The validity of the simulation was confirmed by comparison to the results of E906. For the beryllium target, Fig. 12 shows the agreement between the simulation and the observed spectrum of the outgoing  $K^+$ .

The simulation was used to test the results of the instrumental improvements cited in this proposal by incorporating the modifications of the CDS and studying its response to presumed signal sources as described in the text

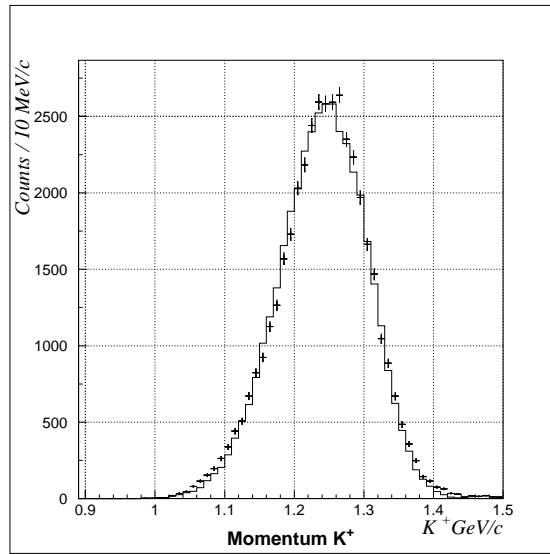


Figure 12: A comparison of the measured and simulated  $K^+$  momentum from the beryllium target



of Section 4.

## C The New Vertex Region Chambers

Two new tracking chambers will be added to the CDS. One is a beam chamber, located just upstream of the target, while the other is a cylindrical detector, designed to yield the z-position of the track at a radius of about 5 cm from the CDC axis. Both chambers are subject to one challenging constraint: The signals they produce must be carried out of the beam pipe without obstruction to both the incident  $K^-$  beam and the out going scattered  $K^+$ 's.

### C.1 Z-Chamber

The z-chamber is a cathode-strip type with cylindrical geometry. A schematic drawing is shown at the top of Fig.13. The wires run parallel to the z-axis (beam direction), and the cathode strips run azimuthally on the outer cathode layer. The cathode layer is produced using multi-layered printed circuit board techniques, and carries the signals out along the outer side of the sheet. The chamber has a flange by which it attaches to the CDC, and on which the preamp circuitry is mounted. The inner cathode is to be made of a carbon-fiber-epoxy composite, and will provide the rigidity and support for the wires. The total thickness of the chamber in the radial direction will be no more than  $0.01 \text{ gr/cm}^2$ .

The required spatial resolution for the z-chamber, as determined from the Monte Carlo simulation is about  $300 \text{ } \mu\text{m}$ , which is readily achievable with cathode-strip type chambers.

### C.2 Beam Tracking Chamber

The beam tracker is a drift chamber consists of six layers (X,X',U,U',V,V') using the well tested design of the beam line chambers used in the D-6 line target area. The main difference is that the signals are carried out of the CDS beam pipe before reaching the preamplifiers. As in the case of the z-chamber, printed circuit board techniques will be employed to construct the pipe which both supports the chamber in place and carries the signals out.

A schematic drawing of this chamber appears at the bottom of Fig. 13. As shown, the planes are circular and laid out in a manner which allows rotation into several possible positions. In particular, a rotation by  $180^\circ$  will create the “primed” plane, offset by half a wire spacing, as required by the standard design. Rotations by  $60^\circ$ ,  $90^\circ$  and  $120^\circ$  are also possible, so that either an  $(X, X', Y, Y')$  or a  $(X, X', U, U', V, V')$  configuration can be used.

The position resolution of the existing chambers with the intended design is  $200\text{ }\mu\text{m}$ . By improving the existing software (the current one uses a constant x-t function), this number can be improved somewhat.

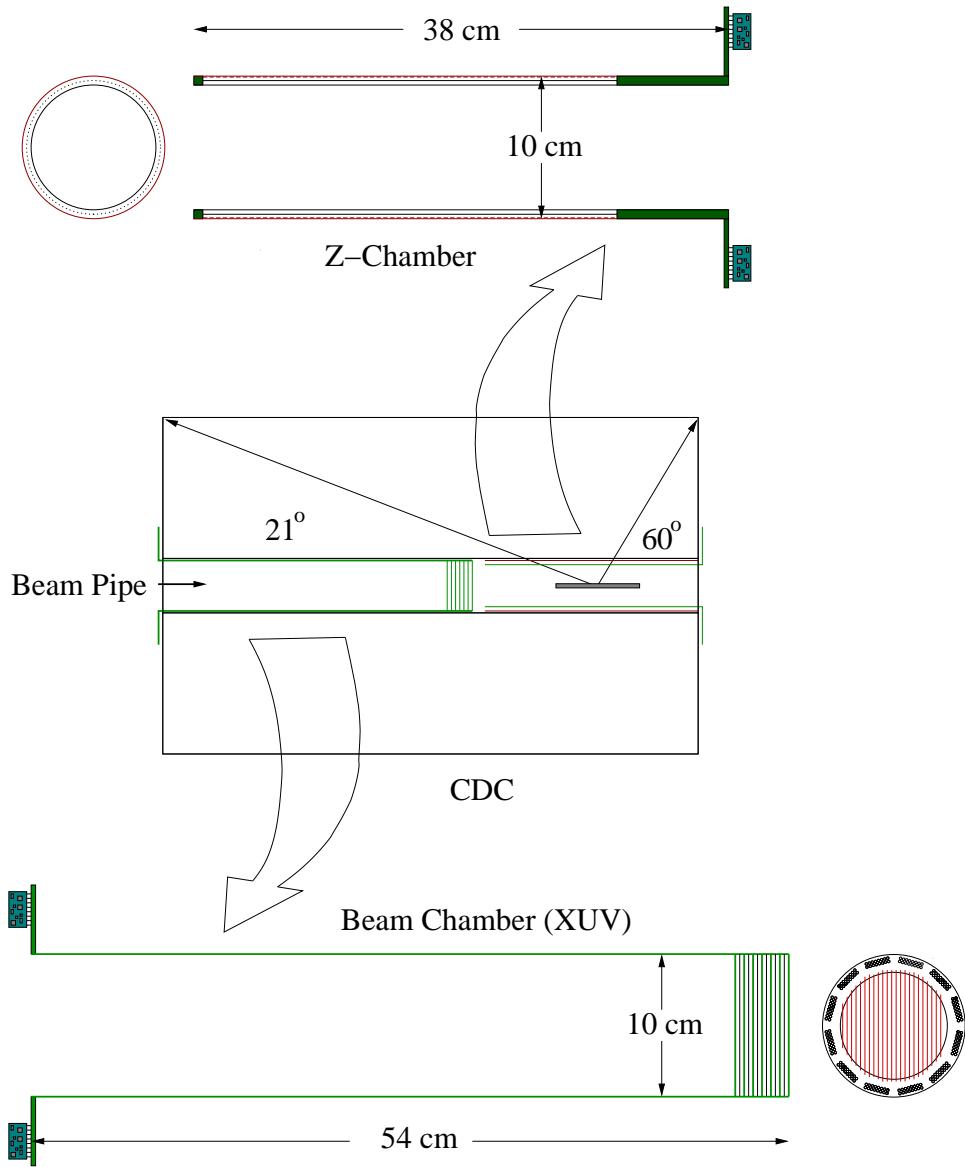


Figure 13: A schematic drawing of the CDC with the target placed in the new position, along with enlarged schematics of the beam-tracking and z chambers. In both cases the signals are carried out on the surface of the G10 or Kapton tube, and the preamplifiers are mounted on the outer flange.

## D Addenda and Corrigenda

In Section 4, a reference to the increase in acceptance (and the resulting increase in event rate) was inadequately described. The increased acceptance results from moving the Be target position downstream 30 cm from the present position. The resulting increase in solid angle was investigated by a simulation. The results show an increase of a factor of 2.4. In order to take advantage of this solid angle increase, some minor adjustments will be made in the spectrometer tune.

At the end of Section 4, the request for beam time contained some incorrect assumptions about how beam time is charged under mode sharing with RHIC operations. The last two sentences now read as follows. For 1000 hours, we will obtain  $(15/7) \times (1000/450) \times (2.4) \times (1/1.07) = 10.7$  times more pion coincident events than obtained in E906. This request asks for an additional 200 hours in setup and calibration time, for a total request of 1200 hours.

The Summary of Section 5 is modified to state we will obtain more than 10 times higher statistics and almost twice better resolution than in E906. The last sentence now reads:

We request 1000 hours at 15 Tp for production and 200 hours at 5 Tp for setup and calibration.

The Proposal Cover sheet is modified to read:

1000 Hours for Production

200 Hours for Setup

The Abstract is modified to claim:  
more than 10 times higher statistics.

## References

- [1] Takatsuka et al., Proc. of the Int. Conf. on Hypernuclear and Strangeness Particle Physics, Torino, Oct 22-26, 2000 (to be published) and Prog. of Theor. Phys. **105**, 179 (2001).
- [2] R. L. Jaffe, Phys. Rev. Lett. **38**, 195 (1977); **38**, 1617(E) (1977)
- [3] M. Danysz et al., Nucl. Phys. **49**, 121 (1963).
- [4] D. J. Prowse, Phys. Rev. Lett. **17**, 782 (1966).
- [5] R. H. Dalitz et al., Proc. R. Soc. Lond. **A426**, 1 (1989).
- [6] S. Aoki et al., Prog. Theor. Phys. **85**, 1287 (1991).
- [7] K. Nakazawa, Proc. of the Int. Conf. on Hypernuclear and Strangeness Particle Physics, Torino, Oct 22-26, 2000 (to be published).
- [8] H. Takahashi et al., submitted to Phys. Rev. C.
- [9] J. Nakano, thesis, University of Tokyo (2000).
- [10] T. Fukuda, R. E. Chrien and A. Rusek, AGS proposal E906 (1994).
- [11] E. Hiyama et al., submitted to Phys. Rev. Lett., preprint nucl-th/0106070.
- [12] P. H. Pile *et al.*, Nucl. Instr. Meth., **A321**, 48 (1992).
- [13] F. Merrill *et al.*, Phys. Rev. **C63**, 035206 (2001).
- [14] Yasuo Yamamoto, Masamichi Wakai, Toshio Motoba and Tomokazu Fukuda, Nucl. Phys. A625 (1997) 107.
- [15] M. Jurič *et al.*, Nucl. Phys. **B52**, 1 (1973).
- [16] G. Bohm *et al.*, Nucl. Phys. **B4**, 511 (1968); see also U. Krecker, D. Kielczewska, and T. Tymieniecka, Nucl. Phys. **A236**, 491, (1974).
- [17] T. Motoba, H. Bando, K. Ikeda, and T. Yamada, Prog. Theor. Phys. Suppl. **81**, 42 (1985).

- [18] T. Motoba, K. Itonaga, and H. Bando, Nucl. Phys. **A 489**, 683 (1988).; T. Motoba, H. Bando, T. Fukuda, and J. Zofka, Nucl. Phys. **A534**, 597 (1991).
- [19] P. Khaustov *et al.*, Phys. Rev. **C61**, 054603 (2000).
- [20] T. Motoba, private communication.
- [21] S. Kahana, private communication.
- [22] GEANT 3.2.1 Detector Description and Simulation Tool, CERN Program Library Long Writeup, 1994.
- [23] Toru Tamagawa, Dissertation, University of Tokyo, 2000.